Advances in Materials Physics and Chemistry, 2021, 11, 67-77
https://www.scirp.org/journal/ampc
ISSN Online: 2162-5328
ISSN Print: 2162-531X

Synthesis and Characterization of SnO_2 Flower-Shaped by Hydrothermal Route for Formaldehyde Sensing Properties

Abeer Alhadi[1], Shuyi Ma[1*], Shitu Pei[1], Tingting Yang[1], Pengdou Yun[1], Qianqian Zhang[1], Hamouda Adam Hamouda[2,3], Li Wang[1], Omer Almamoun[4], Altayeb Alshiply[5], Pengfei Cao[1], Manahil H. Balal[6,7], Khalid Ahmed Abbakar[7,8]

[1]Key Laboratory of Atomic and Molecular Physics & Functional Materials of Gansu Province, College of Physics and Electronic Engineering, Northwest Normal University, Lanzhou, China
[2]College of Chemistry and Chemical Engineering, Northwest Normal University, Lanzhou, China
[3]Department of Chemistry, Faculty of Science, University of Kordofan, El Obeid, Sudan
[4]Faculty of Petroleum and Hydrology Engineering, West Kordofan, Peace University, Almugled, Sudan
[5]Department of Physics, Faculty of Education, University of Khartoum, Khartoum, Sudan
[6]Physics Department, Faculty of Science and Art, Al Baha University, Gilwah, KSA
[7]Department of Mathematics and Physics, Faculty of Education, University of Gadarif, Gadarif, Sudan
[8]College of Mathematics and Statistics, Northwest Normal University, Lanzhou, China

Email: *abeeralhadi18@hotmail.com

How to cite this paper: Alhadi, A., Ma, S.Y., Pei, S.T., Yang, T.T., Yun, P.D., Zhang, Q.Q., Hamouda, H.A., Wang, L., Almamoun, O., Alshiply, A., Cao, P.F., Balal, M.H. and Abbakar, K.A. (2021) Synthesis and Characterization of SnO_2 Flower-Shaped by Hydrothermal Route for Formaldehyde Sensing Properties. *Advances in Materials Physics and Chemistry*, **11**, 67-77.
https://doi.org/10.4236/ampc.2021.114007

Received: March 11, 2021
Accepted: April 3, 2021
Published: April 6, 2021

Abstract

In this work, we've made SnO_2 flower formed with the aid of using easy test steps, and without cost, which is the hydrothermal approach and without a template. We have used a variety of techniques to characterize SnO_2 flower-shaped by (SEM, TEM, XRD, BET and XPS) instruments. Confirmatory tests carried out have proven that the surface of the tetragonal structure of SnO_2 has a rough surface which makes it excellent for its gas-sensing properties. The gas detection test of SnO_2 flower-shaped proved that it possesses the selectivity of formaldehyde gas (about 30), the optimum operating temperature of the sensor is 220˚C, and also the sensor has a high response time and recovery time is (5 s and 22 s) to 100 ppm, respectively. Particularly, the sensor has an obvious response value (2) when exposed to 5 ppm formaldehyde. As well, the mechanism of gas-sensing was also discussed.

Keywords

SnO_2 Flower-Shaped, Hydrothermal Method, Formaldehyde, Semiconductor, Gas Sensor

1. Introduction

VOCs (Volatile organic compounds) are responsible for the odor, scents, and

perfumes as well as pollutants. Some VOCs are very serious matters to human health and cause harm to the environment. Most VOCs are flammable, explosive, and toxic, and are mainly found in the gaseous phase, so they need to be detected to preserve the health of the peoples [1] [2]. Formaldehyde is a form of a volatile organic compound, so it must be disclosed that it is toxic and odorless, and is considered a cause of environmental pollution [3] [4], Formaldehyde is fatal if exposed for short periods of time and exposure to it for a long period's cause's difficulty breathing, as it is a carcinogen [5], It is necessary to find a high-performance sensor to detect formaldehyde gas because it is already internationally classified by the IARC (International Agency for Research on Cancer) [6]. The MOS (metal oxide semiconductor) such as WO_3, ZnO, SnO_2, NiO, Cu_2O, and In_2O_3 have been used due to their stable properties in chemical transport, so it has been widely used for the detection of different kinds of volatile organic compounds [7]. In detail, SnO_2 (n-type) has the best MOS because it has many advantages such as low cost, good stability, ultra-high sensitiveness, also has excellent performance of gas sensors. The flower-like structure can cause vast concern owing to its tailored structure and high surface area, which is applicable for gas adsorption and desorption [8] [9] [10].

Gas sensors based on SnO_2 materials were developed by many researchers, D. P. Xue, Y. W, *et al.* synthesis of SnO_2 sensor to methane by an impregnation route [11], Q. W, P. S *et al.* discussed SnO_2 sensor to find out formaldehyde via hydrothermal technique [12], According to the previous researches, detecting gas sensors to the pure SnO_2 didn't Achieve Gas sensor detection requirements [13] [14] [15] [16], but in our work pure SnO_2 has good sensing materials for gas sensors detecting. In gas-detection SnO_2 sensors have been utilized closely none less, they are usually used at high operating temperatures (above 300˚C). Thus, it is important to create and develop SnO_2 sensors for low-temperature [17].

In this subject, the hydrothermal technique is used to prepare SnO_2 flower-shaped. Various analysis techniques were used to test the SnO_2 sample. Performance of gas sensing has been discussed systematically, like a response to diverse concentrations, response to various gases and response/recovery time. Optimum operating temperature, and stability, Likewise, we studied the gas sensor mechanism. Consequently, the SnO_2 material could be a good new kind of formaldehyde gas sensor in later years.

2. Experimental

In this experiment, all chemicals were used without any further purification, the steps of hydrothermal method are as follows; 0.4 g Tin (II) Chloride dehydrates, 2.5 g Sodium Citrate dehydrate, and 0.3 g Polyvinylpyrrolidone (Mw = 1,300,000) was fully dissolved into 30 mL mingled solution contained deionized water (DI) and ethylene glycol under the magnetic stirring for 1 h at 30˚C until the solution became identical, and then ammonia solution was added till PH = 9. The uniform solution got after the magnetic stirring for 1 hour. Then solution trans-

ferred to Teflon-lined stainless-steel autoclave, and then heated in a stove at 180˚C for 20 h, and Cooled down to room temperature normally. Next, the Precipitates by centrifugation were washed four times with ethanol and (DI), one by one, next, the sample dried up at 60˚C for 24 h. lastly, SnO_2 flower-shaped were obtained through annealing process in a furnace at 400˚C for 2 h at a ramping rate of 10˚C/min.

Morphological analysis was carried out by Field-emission scanning electron microscopy (SEM, S-4800) and transmission electron microscopy (TEM, USA FEI TEVNAI G2 TF20). The specific surface area was analyzed by Brunauer-Emmett-Teller (BET) method through nitrogen adsorption using the BK132F instrument. The crystalline structure of SnO_2 flower-shaped was determined by X-ray diffraction (XRD, D/Max-2400) using Cu Kα1 radiation with λ = 1.5406 Å, X-ray Photoelectron Spectroscopy (XPS, ESLALAB 220-XL) were examined the elemental composition and chemical state of SnO_2 flower-shaped.

We tested the properties of the gas-sensing using a WS-30A gas sensing measurement system (Wei Sheng Electronics Science and Technology Co., Ltd., Henan Province, China).

The response value (R) was defined as R_a/R_g, where R_a and R_g were the resistance of the sensor in the air and in the test gas, respectively [18] [19]. The response and recovery times are defined as the time required to reach 90% of the final equilibrium value [20] [21].

We put a little of the powder obtained after calcination the process on a glass slide and mixed it with DI water to form clay, next, the slurry uniformly pasted with a toothpick onto a ceramic tube surface. Finally, the sensor was dried naturally at 24 h and was antiquated for 72 h to improve the stability [22], Ni-Cr heating wire played a vital role to adjust the operating temperature (**Figure 1(a)**).

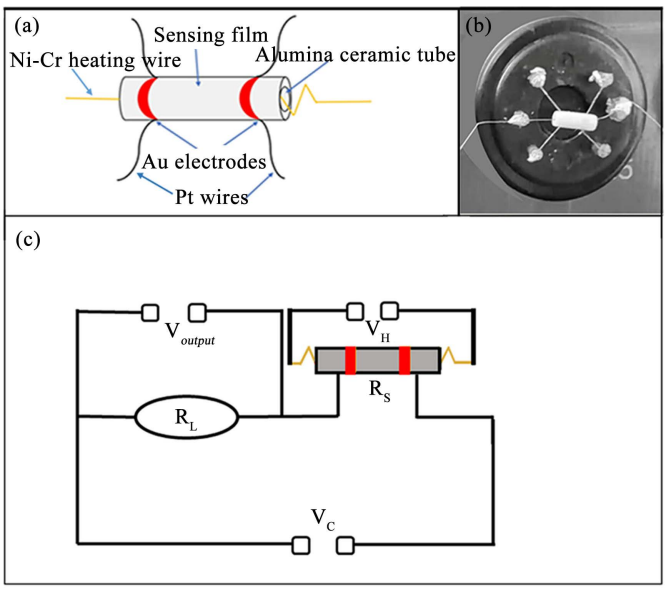

Figure 1. Graphic explanation of gas sensing device, ((a), (b)) the gas sensor and (c) the electrical circuit for gas sensing device.

Figure 1(c) showed that load resistor (R_L) and ready sensor have been tuned and were connected with DC power at 5 V in a gas sensing device. Then, it was selected (R_L) and tuning by (V_H) and was controlled the temperature of the Ni-Cr wire, in Figure 1(b), After inserting the sensor into the test room, the liquid was sprayed into the chamber (with 18 L volume) by the syringe according to the target gas concentrations, and there are also two fans for easy gas dispersion in the test room.

3. Results and Discussion

Figure 2 shows XRD patterns of SnO_2 flower-shaped, it matches well all the diffraction peaks to the tetragonal rutile SnO_2, which were indexed by the standard card (JCPDS, 41-1445) with a = b = 4.736 Å and c = 3.185 Å. That denotes a high crystallinity of the sample after calcining at 500˚C for 3 h. further, there is no impurity phase showed which indicates the prepared SnO_2 was in high purity.

The nanosheets are become gathered and uniform by helping of PVP (Figure 3(a)), all the flower-shaped collected look like similar nanosheets with diameters of about 1 μm. Figure 3(b) showed that our sample is 3D nanostructures. Figure 3(c) and Figure 3(d) presented TEM images, the diameter of flower-shaped microstructures is 4 μm, and it is matching with SEM results. Besides, the rim portion of the flower-shaped structures is very clear because of the unique structures of nanosheets, Also uniform nanosheets are rough, which it's good for desorption and adsorption of gas molecules, subsequently, gas sensing improvement [23].

Meanwhile, the HRTEM image shown in Figure 3(e) the lattice distances of SnO_2 flower-shaped are 0.232 nm and 0.267 nm, it matched well with (200) (101) crystallographic orientation.

What's more, the inner figure in Figure 3(e) is the SAED pattern detected polycrystalline SnO_2 nanostructures.

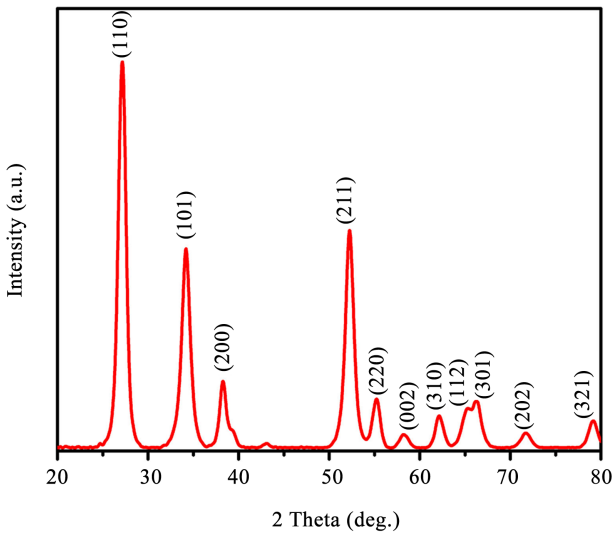

Figure 2. The XRD pattern of SnO_2 flower-shaped.

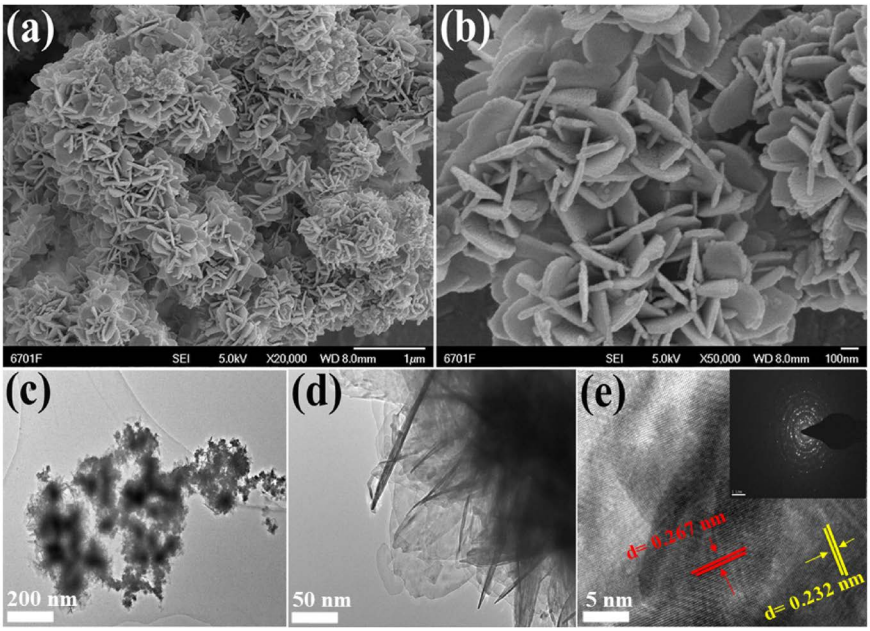

Figure 3. The morphologies of SnO_2 flower-shaped: (a) The low enlargement SEM picture of SnO_2 flower-shaped; and (b) The high enlargement SEM picture of SnO_2 flower-shaped; ((c), (d)) The TEM picture of SnO_2 flower-shaped; (e) The HRTEM picture of SnO_2 flower-shaped, the inner figure in **Figure 3(e)** is SAED pattern.

Figure 4(a) displayed N desorption-adsorption of SnO_2 sample, the BJH pore size is 30 nm and the surface area (BET) of SnO_2 sample is 23.53 m^2/g. Generally, a great pore size is useful to gas disperse, also, a great surface area to supply more active sites, so this leads to improving gas sensing capability [24] [25]. **Figures 4(b)-(d)** presented XPS of SnO_2 for the purpose of examining the elements and their corresponding valence state. The XPS broad spectrum showed the peaks of Sn, O, and C elements in the sample suggesting Sn has successfully co-operated toward the SnO_2.

In **Figure 4(c)**, the binding energies of Sn 3d established to 495.2 and 486.7 eV peaks and are compatible with Sn $3d_{5/2}$ and Sn $3d_{3/2}$ binding energies, respectively that is pointed out typical oxidation valence phase of Sn^{4+} [26] (**Figure 4(d)**). The binding energies of O 1s separated at 530.6 eV, 531.8 peaks. And matched well to crystal lattice oxygen and adsorption oxygen, respectively [27], when the optimal operating temperature increasing, in **Figure 5(a)**, the response of the gas sensor increases gradually until getting to the max value of 30 at 220˚C and then decrease, and were calculated to 100 ppm HCHO, this incident could be simply explained by the kinetics and thermodynamics of gas adsorption and desorption on the surface of the sensing layer [28] [29] from **Figure 5(a)**, the optimal operating temperature of the sample is 220˚C Also. As long as, in **Figure 5(b)**, the response of the gas sensors application was very significant, and it was measured with different concentrations of formaldehyde (5, 15, 25, 50, 100, 150, 200, 500 and 1000 ppm), when the formaldehyde concentration increases that means the response gradually going to increase the gas sensor almost be

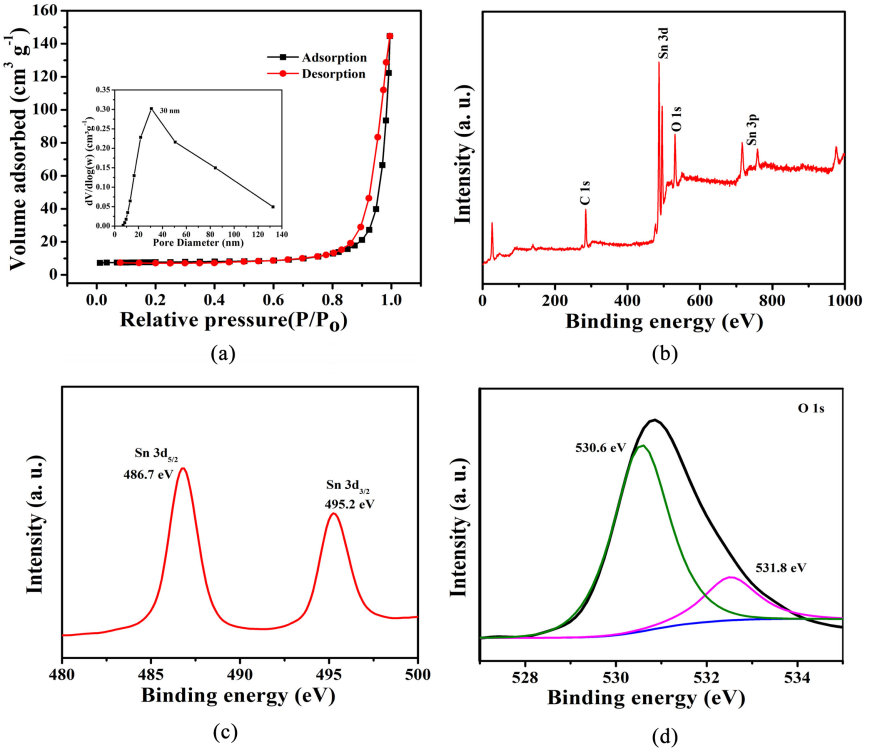

Figure 4. (a) N_2 desorption-adsorption of SnO_2 flower-shaped and the inner figure is pore-size distribution curves obtained by BJH method, XPS spectra of the SnO_2; (b) a survey spectrum; (c) Sn 3d; (d) O 1s.

stable when the concentration is above 200 ppm, which means It connects the responses with the low concentrations. The dynamic response/recovery times of (3D) SnO_2 flower-shaped exhibited in **Figure 5(c)** for different concentrations (15, 25, 50, 100, and 200) ppm at 220˚C for HCHO, we can obviously see that the response increases gradually with an increasing concentration of HCHO. This shows that our sensor can show a significant response (about 7 for Formaldehyde), while the gas concentration is low (15 ppm). That leads to sensing properties of the sample (3D) SnO_2 flower-shaped is good. **Figure 5(d)** the response/recovery times to 50 ppm formaldehyde about 5 s and 22 s respectively. The rough surface has a significant role in short recovery and response times. the selectivity of the sample is a necessary role for the performance of gas sensing, the selectivity of the sample was examined to different gasses in **Figure 5(e)** displayed Our sensor is high selectivity to formaldehyde, **Figure 5(f)** we have tested the stability of the sample in a few days, which clarified that our sample is gradually stable. Also, **Table 1** summarized comparison between this work and previous works reported.

The mechanism of the SnO_2 sample was also investigated in **Figure 6**. (Ammonia, Polyvinylpyrrolidone and sodium citrate) are a key factor affecting the morphology growth in good shape, the $NH_3{\cdot}H_2O$ can release OH^- as a low alkaline solution that reacts with Sn^{2+}, thus its control the final SnO_2 flower-shaped [35]. In the next equations, we explain that:

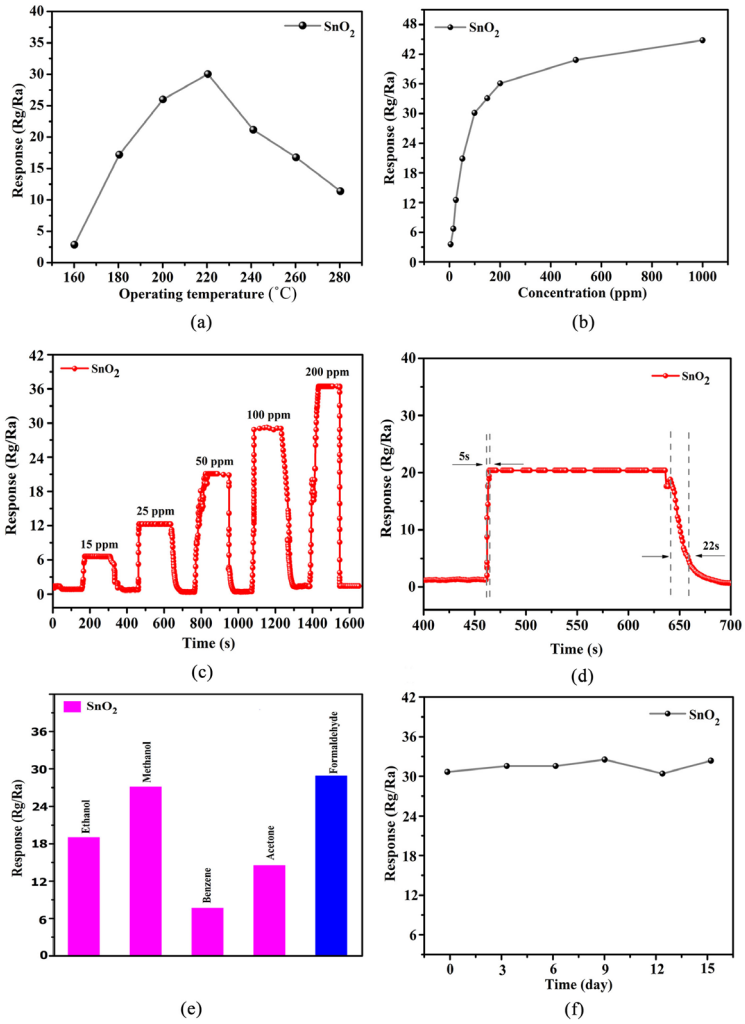

Figure 5. (a) gas sensor responses of sample to 100 ppm HCHO to different operating temperatures; (b) gas sensor responses to different concentrations (5 - 1000 ppm) of HCHO; (c) The response/recovery time to 15, 25, 50, 100, 200, ppm HCHO; (d) the response and recover time towards 50 ppm HCHO at 220˚C; (e) The responses of SnO_2 sample to 100 ppm various test gases; (f) The stability of SnO_2 sample to 100 ppm HCHO at 220˚C.

Table 1. Showed a comparison of various SnO_2 sensors between published work and this work.

Sensor materials	Con (ppm)	Selectivity	Gas response	Synthetic method	Ref.
Porous SnO_2 nanowires	100	ethanol	~1.7	EF, HM	[30]
GO/SnO_2 nanosheets	100	ethanol	2.9	HM	[31]
WO_3-SnO_2 nanosphere	1000	acetone	16.9	HM	[32]
La-doped SnO_2 nanoparticles	5	formaldehyde	4.2	BM	[33]
Porous flower-like SnO_2	100	formaldehyde, ethanol	24.8	HM	[34]
SnO_2 flower-shaped	100	formaldehyde	30.0	HM	this work

Where: EF = electrospinning followed, HM = hydrothermal method, BM = Ball-milling solid chemical reaction method.

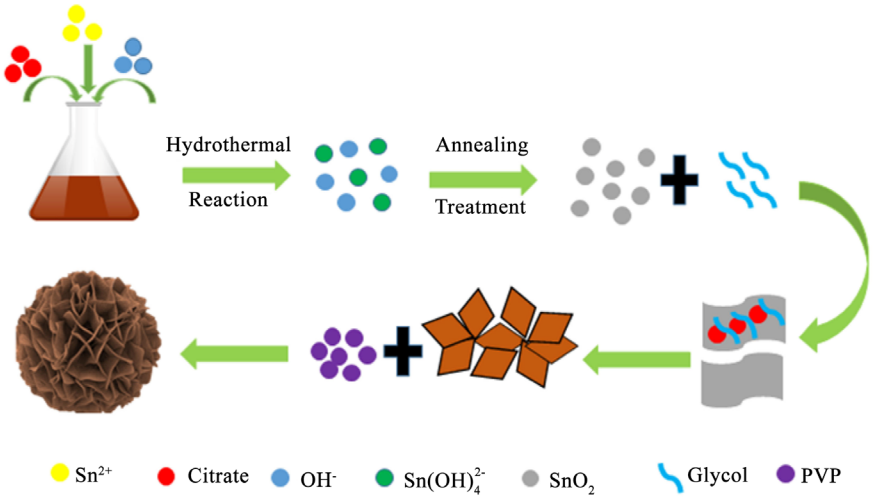

Figure 6. Gas sensing mechanism of SnO_2 flower-shaped.

$$NH_3 \cdot H_2O \rightarrow NH_4^+ + OH^- \quad \text{(a)}$$

$$Sn^{2+} + 4OH^- \rightarrow Sn(OH)_4^{2-} \quad \text{(b)}$$

$$Sn(OH)_4^{2-} \rightarrow SnO_2 + 2H_2O + 2e^- \quad \text{(c)}$$

While the nanosheets increase more separately, individually and uniformly due to PVP, the growth of SnO_2 nanosheets and accelerate the gathering of nanosheets into flower-shaped by sodium citrate [36].

4. Conclusion

The pure SnO_2 flower-shaped was fabricated through the hydrothermal method, the sensor has good sensitivity, stability, high response (30 s), and excellent selectivity to formaldehyde at 220˚C, and a high response/recovery time about (5 s and 22 s). Also, the mechanism of SnO_2 gas sensors is also discussed. Thus, the SnO_2 could become a promising gas sensing material to formaldehyde.

Acknowledgements

This work was supported by the National Natural Science Foundation of China (Grant No. 11864034 and 11964035), and the Scientific Research Project of Gansu Province (Grant No. 18JR3RA089 and 17JR5RA072).

Conflicts of Interest

The authors declare that they have no known competing financial interests or personal relationships that could have appeared to influence the work reported in this paper.

References

[1] Pei, S., Ma, S., Xu, X., Xu, X. and Almamoun. O. (2021) Modulated $PrFeO_3$ by Doping Sm^{3+} for Enhanced Acetone Sensing Properties. *Journal of Alloys and*

Compounds, **856**, Article ID: 158274. https://doi.org/10.1016/j.jallcom.2020.158274

[2] Yang, T.T., Ma, S.Y., Cao, P.F., Xu, X.L., Wang, L., Pei, S.T., *et al.* (2021) Synthesis and Characterization of $ErFeO_3$ Nanoparticles by a Hydrothermal Method for Isopropanol Sensing Properties. *Vacuum*, **185**, Article ID: 110005. https://doi.org/10.1016/j.vacuum.2020.110005

[3] Tie, Y., Ma, S.Y., Pei, S.T., Zhang, Q.X., Zhu, K.M., Zhang, R., *et al.* (2020) Pr Doped $BiFeO_3$ Hollow Nano Fibers via Electrospinning Method as a Formaldehyde Sensor. *Sensors and Actuators B*: *Chemical*, **308**, Article ID: 127689. https://doi.org/10.1016/j.snb.2020.127689

[4] Zhang, G.H., Chen, Q., Deng, X.Y., Jiao, H.Y., Wang, P.Y. and Gengzang, D.J. (2019) Synthesis and Characterization of In-Doped $LaFeO_3$ Hollow Nanofibers with Enhanced Formaldehyde Sensing Properties. *Materials Letters*, **236**, 229-232. https://doi.org/10.1016/j.matlet.2018.10.062

[5] Zhang, R., Ma, S.Y., Zhang, Q.X., Zhu, K.M., Tie, Y., Pei, S.T., *et al.* (2019) Highly Sensitive Formaldehyde Gas Sensors Based on Ag Doped Zn_2SnO_4/SnO_2 Hollow Nanospheres. *Materials Letters*, **254**, 178-181. https://doi.org/10.1016/j.matlet.2019.07.065

[6] Zhu, K.M., Ma, S.Y., Pei, S.T., Tie, Y., Zhang, Q.X., Wang, W.Q., *et al.* (2019) Preparation, Characterization and Formaldehyde Gas Sensing Properties of Walnut-shaped $BiFeO_3$ Microspheres. *Materials Letters*, **246**, 107-110. https://doi.org/10.1016/j.matlet.2019.02.129

[7] Fu, X., Yang, P., Xiao, X., Zhou, D., Huang, R., Zhang, X., *et al.* (2019) Ultra-Fast and Highly Selective Room-Temperature Formaldehyde Gas Sensing of Pt-Decorated MoO_3 Nanobelts. *Journal of Alloys and Compounds*, **797**, 666-675. https://doi.org/10.1016/j.jallcom.2019.05.145

[8] Liu, F., Chen, X., Wang, X., Han, Y., Song, X., Tian, J., *et al.* (2019) Fabrication of 1D Zn_2SnO_4 Nanowire and 2D ZnO Nanosheet Hybrid Hierarchical Structures for Use in Triethylamine Gas Sensors. *Sensors and Actuators B*: *Chemical*, **291**, 155-163. https://doi.org/10.1016/j.snb.2019.04.009

[9] Xue, D., Zhang, Z. and Wang, Y. (2019) Enhanced Methane Sensing Performance of SnO_2 Nanoflowers Based Sensors Decorated with Au Nanoparticles. *Materials Chemistry and Physics*, **237**, Article ID: 121864. https://doi.org/10.1016/j.matchemphys.2019.121864

[10] Wang, X., Liu, F., Chen, X., Lu, G., Song, X., Tian, J., *et al.* (2020) SnO_2 Core-Shell Hollow Microspheres Co-Modification with Au and NiO Nanoparticles for Acetone Gas Sensing. *Powder Technology*, **364**, 159-166. https://doi.org/10.1016/j.powtec.2020.02.006

[11] Xue, D., Wang, Y., Cao, J., Sun, G. and Zhang, Z. (2019) Improving Methane Gas Sensing Performance of Flower-Like SnO_2 Decorated by WO_3 Nanoplates. *Talanta*, **199**, 603-611. https://doi.org/10.1016/j.talanta.2019.03.014

[12] Wei, Q., Song, P., Li, Z., Yang, Z. and Wang, Q. (2017) Hierarchical Peony-Like Sb-Doped SnO_2 Nanostructures: Synthesis, Characterization and HCHO Sensing Properties. *Materials Letters*, **191**, 173-177. https://doi.org/10.1016/j.matlet.2016.12.070

[13] Cao, J., Qin, C., Wang, Y., Zhang, H., Zhang, B., Gong, Y., *et al.* (2017) Synthesis of G-C_3N_4 Nanosheet Modified SnO_2 Composites with Improved Performance for Ethanol Gas Sensing. *RSC Advances*, **7**, 25504-25511. https://doi.org/10.1039/C7RA01901G

[14] Chen, W.C., Foxley, S. and Miller, K.L. (2013) Detecting Microstructural Properties

of White Matter Based on Compartmentalization of Magnetic Susceptibility. *NeuroImage*, **70**, 1-9. https://doi.org/10.1016/j.neuroimage.2012.12.032

[15] Kim, K.M., Choi, K.I, Jeong, H.M., Kim, H.J., Kim, H.R. and Lee, J.H. (2012) Highly Sensitive and Selective Trimethylamine Sensors Using Ru-Doped SnO_2 Hollow Spheres. *Sensors and Actuators B*: *Chemical*, **166**-**167**, 733-738. https://doi.org/10.1016/j.snb.2012.03.049

[16] Wang, D., Chu, X. and Gong, M. (2006) Gas-Sensing Properties of Sensors Based on Single-Crystalline SnO_2 Nanorods Prepared by a Simple Molten-Salt Method. *Sensors and Actuators B*: *Chemical*, **117**, 183-187. https://doi.org/10.1016/j.snb.2005.11.022

[17] Hoefer, U., Frank, J. and Fleischer, M. (2001) High Temperature Ga2O3-Gas Sensors and SnO_2-Gas Sensors: A Comparison. *Sensors and Actuators B*: *Chemical*, **78**, 6-11. https://doi.org/10.1016/S0925-4005(01)00784-5

[18] Ma, L., Ma, S.Y., Shen, X.F., Wang, T.T., Jiang, X.H., Chen, Q., *et al.* (2018) $PrFeO_3$ Hollow Nanofibers as a Highly Efficient Gas Sensor for Acetone Detection. *Sensors and Actuators B*: *Chemical*, **255**, 2546-2554. https://doi.org/10.1016/j.snb.2017.09.060

[19] Chen, Q., Ma, S.Y., Xu, X.L., Jiao, H.Y., Zhang, G.H., Liu, L.W., *et al.* (2018) Optimization Ethanol Detection Performance Manifested by Gas Sensor Based on In_2O_3/ZnS Rough Microspheres. *Sensors and Actuators B*: *Chemical*, **264**, 263-278. https://doi.org/10.1016/j.snb.2018.02.172

[20] Cao, P.F., Ma, S.Y., Xu, X.L., Wang, B.J., Almamoun, O., Han, T., *et al.* (2020) Preparation and Characterization of a Novel Ethanol Gas Sensor Based on $FeYO_3$ Microspheres by Using Orange Peels as Bio-Templates. *Vacuum*, **177**, Article ID: 109359. https://doi.org/10.1016/j.vacuum.2020.109359

[21] Lu, J., Liang, K., Xu, C., Wang, X., Ouyang, H., Huang, J., *et al.* (2019) Humidity Sensor Based on heterogeneous $CoTiO_3$/TiO_2 Film with Vertically Aligned Nanocrystalline Structure. *Vacuum*, **163**, 292-300. https://doi.org/10.1016/j.vacuum.2019.02.027

[22] Kapse ,V.D., Ghosh, S.A., Chaudhari, G.N., Raghuwanshi, F.C. and Gulwade, D.D. (2008) H2S Sensing Properties of La-Doped Nanocrystalline In_2O_3. *Vacuum*, **83**, 346-352. https://doi.org/10.1016/j.vacuum.2008.05.027

[23] Jin, W.X., Ma, S.Y., Tie, Z.Z., Wei, J.J., Luo, J., Jiang, X.H., *et al.* (2015) One-Step Synthesis and Highly Gas-Sensing Properties of Hierarchical Cu-Doped SnO_2 Nanoflowers. *Sensors and Actuators B*: *Chemical*, **213**, 171-180. https://doi.org/10.1016/j.snb.2015.02.075

[24] Li, J., Fan, H. and Jia, X. (2010) Multilayered ZnO Nanosheets with 3D Porous Architectures: Synthesis and Gas Sensing Application. *The Journal of Physical Chemistry C*, **114**, 14684-14691. https://doi.org/10.1021/jp100792c

[25] Yang, D. and Liu, Z. (2007) One-Dimensional Nanostructures of Silicon: Synthesis, Characterization and Applications. *ChemInform*, **39**, 95-110.

[26] Ge, H., Wang, C. and Yin, L. (2015) Hierarchical $Cu_{0.27}Co_{2.73}O_4$/MnO_2 Nanorod Arrays Grown on 3D Nickel Foam as Promising Electrode Materials for Electrochemical Capacitors. *Journal of Materials Chemistry A*, **3**, 17359-17368. https://doi.org/10.1039/C5TA03049H

[27] Zhang, R., Xu, Z., Zhou, T., Fei, T., Wang, R. and Zhang, T. (2019) Improvement of Gas Sensing Performance for Tin Dioxide Sensor through Construction of Nanostructures. *Journal of Colloid and Interface Science*, **557**, 673-682. https://doi.org/10.1016/j.jcis.2019.09.073

[28] Cao, J., Zhang, H. and Yan, X. (2016) Facile Fabrication and Enhanced Formaldehyde Gas Sensing Properties of Nanoparticles-Assembled Chain-Like NiO Architectures. *Materials Letters*, **185**, 40-42. https://doi.org/10.1016/j.matlet.2016.08.099

[29] Wei, Q., Sun, J., Song, P., Li, J., Yang, Z. and Wang, Q. (2020) MOF-Derived α-Fe_2O_3 Porous Spindle Combined with Reduced Graphene Oxide for Improvement of TEA Sensing Performance. *Sensors and Actuators B*: *Chemical*, **304**, Article ID: 127306. https://doi.org/10.1016/j.snb.2019.127306

[30] Li, R., Chen, S., Lou, Z., Li, L., Huang, T., Song, Y., *et al.* (2017) Fabrication of Porous SnO_2 Nanowires Gas Sensors with Enhanced Sensitivity. *Sensors and Actuators B*: *Chemical*, **252**, 79-85. https://doi.org/10.1016/j.snb.2017.05.161

[31] Zhao, C., Gong, H., Lan, W., Ramachandran, R., Xu, H., Liu, S., *et al.* (2018) Facile Synthesis of SnO2 Hierarchical Porous Nanosheets from Graphene Oxide Sacrificial Scaffolds for high-Performance Gas Sensors. *Sensors and Actuators B*: *Chemical*, **258**, 492-500. https://doi.org/10.1016/j.snb.2017.11.167

[32] Zhu, Y., Wang, H., Liu, J., Yin, M., Yu, L., Zhou, J., *et al.* (2019) High-Performance Gas Sensors Based on the WO_3-SnO_2 Nanosphere Composites. *Journal of Alloys and Compounds*, **782**, 789-795. https://doi.org/10.1016/j.jallcom.2018.12.178

[33] Xiang, X., Zhu, D. and Wang, D. (2016) Enhanced Formaldehyde Gas Sensing Properties of La-Doped SnO_2 Nanoparticles Prepared by Ball-Milling Solid Chemical Reaction Method. *Journal of Materials Science*: *Materials in Electronics*, **27**, 7425-7432. https://doi.org/10.1007/s10854-016-4718-8

[34] Ren, H., Zhao, W., Wang, L., Ryu, S.O. and Gu, C. (2015) Preparation of Porous Flower-Like SnO_2 Micro/Nano Structures and Their Enhanced Gas Sensing Property. *Journal of Alloys and Compounds*, **653**, 611-618. https://doi.org/10.1016/j.jallcom.2015.09.065

[35] Suwanboon, S., Amornpitoksuk, P. and Muensit, N. (2011) Dependence of Photocatalytic Activity on Structural and Optical Properties of Nanocrystalline ZnO Powders. *Ceramics International*, **37**, 2247-2253. https://doi.org/10.1016/j.ceramint.2011.03.016

[36] Luo, J., Ma, S.Y., Li, F.M., Li, X.B., Li, W.Q., Cheng, L., *et al.* (2014) The Mesoscopic Structure of Flower-Like ZnO Nanorods for Acetone Detection. *Materials Letters*, **121**, 137-140. https://doi.org/10.1016/j.matlet.2014.01.155